

# Deformation structures and an alteration zone linked to deposition of volcanogenic sulphate in an ancient playa (Oligocene of Nebraska, USA)

DAVID B. LOOPE\*, JOSEPH A. MASON†, HUIMING BAO‡, RICHARD M. KETTLER\* and C. WILLIAM ZANNER¶

\*Department of Geosciences, University of Nebraska, Lincoln NE 68588–0340, USA (E-mail: [dloope1@unl.edu](mailto:dloope1@unl.edu))

†Conservation & Survey Division and Department of Geosciences, University of Nebraska, Lincoln NE 68588–0340, USA

‡Department of Geology and Geophysics, Louisiana State University, Baton Rouge, LA 70803, USA

¶School of Natural Resources, University of Nebraska, Lincoln NE 68588–0915, USA

## ABSTRACT

Historic, sulphur-rich volcanic eruptions have altered global climate for as much as five years, and much larger events are known from the geologic record. At Scotts Bluff, Nebraska, Early Oligocene strata of the lower Arikaree Group contain a tephra bed with abundant calcite pseudomorphs after gypsum. Previous work has shown sulphate from the pseudomorphs in this tephra bears a high  $^{17}\text{O}$  anomaly indicative of oxidation of sulphur gases by ozone or hydrogen peroxide in the atmosphere. Possible sources of the tephra were caldera eruptions at about 28 Ma in the San Juan volcanic field of southwestern Colorado (~500 km SW of the study site) and the eastern Great Basin (~1000 km WSW). The present sedimentological study shows that tephra and volcanogenic sulphate were deposited and preserved within a small, surface-discharging playa that developed on the irregular upper surface of aeolian siltstones of the subjacent White River Group. Sulphate solutions (including perhaps sulphuric acid) percolated downward within the vadose zone, dissolving early formed smectite cement within underlying volcanoclastic sandstones, reddening these rocks along an irregular alteration front. Preserved fine-scale stratification within the sandstones precludes the possibility that reddening took place during pedogenesis. Displacive growth of gypsum at the playa centre folded tephra beds and forced tephra into underlying sandstones, forming elongate cones. The large mass fraction of gypsum (now replaced by calcite) in the playa sediments suggests a huge, long-distance delivery of sulphate aerosols. Some of the sulphate and tephra may have come from the same eruption, or the fine-grained tephra may simply have aided preservation of dry-fog sulphate derived from an unrelated, effusive eruption of lava.

**Keywords** Gypsum, Nebraska, Oligocene, playa, tephra, volcanogenic sulphate.

## INTRODUCTION

During 1783 and 1784, a prolonged, effusive eruption of about  $15 \text{ km}^3$  of basaltic magma from Laki on Iceland released 122 megatons of  $\text{SO}_2$  and generated a sulphate aerosol (dry fog) that envel-

oped the northern hemisphere above the 35th parallel for more than five months (Grattan & Pyatt, 1994; Stothers, 1996; Thordarson & Self, 2003). Historic, sulphur-rich volcanic eruptions have altered global climate for as much as five years, and much larger events are known from the

geological record (Stothers, 1984; Devine *et al.*, 1984; Thordarson & Self, 1996; Yasui *et al.*, 1996; Robock, 2000; Thordarson *et al.*, 2003). Although evidence exists for volcanic eruptions several hundreds of times the volume of Laki, geochemical evidence of pre-Quaternary dry-fog deposition events had not been reported until Bao *et al.* (2000) showed that sulphate ions washed from calcite pseudomorphs after gypsum within silicic Oligocene tephra at Scotts Bluff on the High Plains of westernmost Nebraska bear a highly positive  $^{17}\text{O}$  anomaly. The anomaly is indicative of atmospheric oxidation of sulphur gases by ozone or hydrogen peroxide. Sulphur isotope ratios from the Scotts Bluff tephra are near zero or slightly positive. This is consistent with a volcanic origin, but inconsistent with derivation from groundwater or dust from the Pierre Shale (Cretaceous) which underlies Cenozoic rocks in the Scotts Bluff area and crops out extensively on the central and northern Great Plains. Important conclusions of a more recent study (Bao *et al.*, 2003) are that: (1) the sulphate washed from freshly collected samples of recent volcanic ash does not carry an isotopic anomaly, and (2) the isotopic anomaly at Scotts Bluff was probably a product of extreme dry fog (sulphate haze) events similar to those produced by the Laki eruptions.

One purpose of this paper is to describe an alteration zone and three kinds of unusual deformation structures that lie below the airfall tephra at Scotts Bluff and to offer a geomorphic-hydrologic interpretation that is consistent with this sedimentologic evidence, and with the isotopic data of Bao *et al.* (2000, 2003). Another purpose is to explain the conditions that led to preservation of this distinctive (but rare) isotopic signature. The Great Plains of North America is one of the windiest non-maritime regions in the world, and thousands of closed, deflationary basins (playas) mark its surface (Holliday in Osterkamp *et al.*, 1987). One conclusion of this study is that the deformation of the Oligocene strata took place when gypsum grew just below the surface of a small, surface-water discharging playa (see classification by Motts, 1965) that was closely analogous to the playas on the modern Great Plains. The Oligocene strata were chemically altered during a relatively short interval when alkaline pore waters were strongly modified by the far-travelled sulphuric acid. In the small playa setting, the  $^{17}\text{O}$  anomaly was not lost through dilution by surface water or groundwater, and organic matter was sufficiently sparse to limit the effects of sulphate-reducing bacteria.

Preservation of the  $^{17}\text{O}$ -anomalous sulphate (Bao *et al.*, 2000, 2003) requires that several specific conditions must have prevailed in the depositional and subsurface environments. Within modern Great Plains streams and aquifers, the Late Cretaceous Pierre Shale is the major source of sulphate in groundwater. This sulphate, largely derived from oxidation of pyrite in the marine mudstone facies, has widely varying  $\delta^{34}\text{S}$  values and no  $^{17}\text{O}$  anomaly. For example, in north-western Nebraska, a  $\sim 15$  m-thick deposit of Eocene gypsum rests directly on the paleosol developed at the upper surface of the Pierre Shale. Data from this deposit show that none of the different layers of gypsum has an  $^{17}\text{O}$  anomaly, and that the  $\delta^{34}\text{S}$  ranges from 12.2 to 14.8‰ ( $n = 11$ ). Although the initial sulphate derived from the oxidation of synsedimentary pyrite has a strongly negative  $\delta^{34}\text{S}$  value (Gautier, 1987), subsequent microbial reduction apparently increased the  $\delta^{34}\text{S}$  of sulphate remaining in the system. At Scotts Bluff, however,  $\delta^{34}\text{S}$  within sulphates leached from the airfall tephra and the reworked facies are near zero or slightly positive, consistent with a volcanogenic source, and the  $^{17}\text{O}$  anomalies are highly positive, indicating oxidation of sulphur gases in the atmosphere (Bao *et al.*, 2003; Table 1).

This study leaves an important issue unresolved: Although the dry fogs studied to date (e.g. Thordarson & Self, 2003) are products of long-duration, effusive eruptions of basaltic lava, the isotopic anomaly at Scotts Bluff is from a silicic tephra. Future studies should address the possibility that silicic eruptions can also generate widespread, tropospheric dry fogs.

## GEOLOGIC SETTING

### Study area and stratigraphy

An enormous volume of chiefly silt-to-sand sized volcanoclastic sediments accumulated in the North American mid-continent and adjacent Rocky Mountain basins from the Late Eocene to the Early Miocene ( $\sim 37$ –19 Ma; Terry *et al.*, 1998). On the central Great Plains during this interval, debris from eruptive centres in the Great Basin and southern Rocky Mountains was mixed with quartz-rich epiclastic material by eastward-flowing streams and westerly winds. Weakly lithified strata of the White River and Arikaree Groups that contain an abundant and diverse assemblage of Mid-Tertiary mammals are now

widely exposed in the headwaters of the Platte and Missouri Rivers.

This study focuses on steep exposures that form the walls of Scotts Bluff, a butte in westernmost Nebraska with an areal extent of less than 1 km<sup>2</sup> (Fig. 1). Within the study area, very-fine-grained volcanoclastic sandstones of the Upper Oligocene Gering Formation (Arikaree Group) rest on volcanoclastic siltstones of the Upper Oligocene Brule Formation (White River Group, Fig. 2). Reworked glass is a major component in both formations (Swinehart *et al.*, 1985), and thin beds of airfall tephra are prominent in the lower part of the Gering Formation. Tedford *et al.* (1996) considered the depositional environment of the Gering Formation at Scotts Bluff to be a playa – an interpretation that is supported by this study. The closed hydrographic basin that supported the

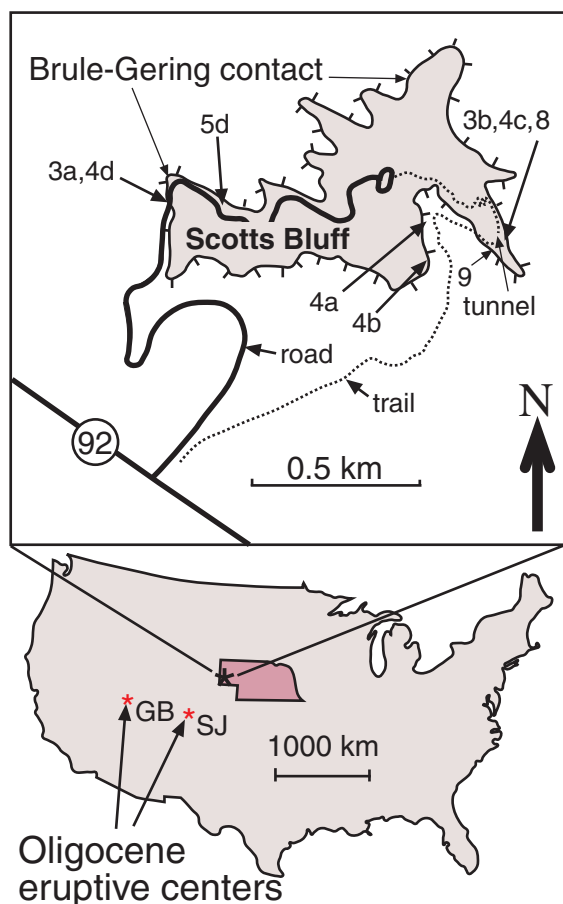


**Fig. 1.** The study area encompasses Scotts Bluff, a butte in westernmost Nebraska, USA. The contact between the Brule and Gering Formations lies near the 4400 foot contour line (Scotts Bluff South Quadrangle, 7.5 Minute Series). Numbers relate to figures in text. The most likely sources of the Scotts Bluff tephra are Oligocene (about 28 Ma) eruptive centres in the Great Basin (GB), and the San Juan Volcanic Field (SJ).

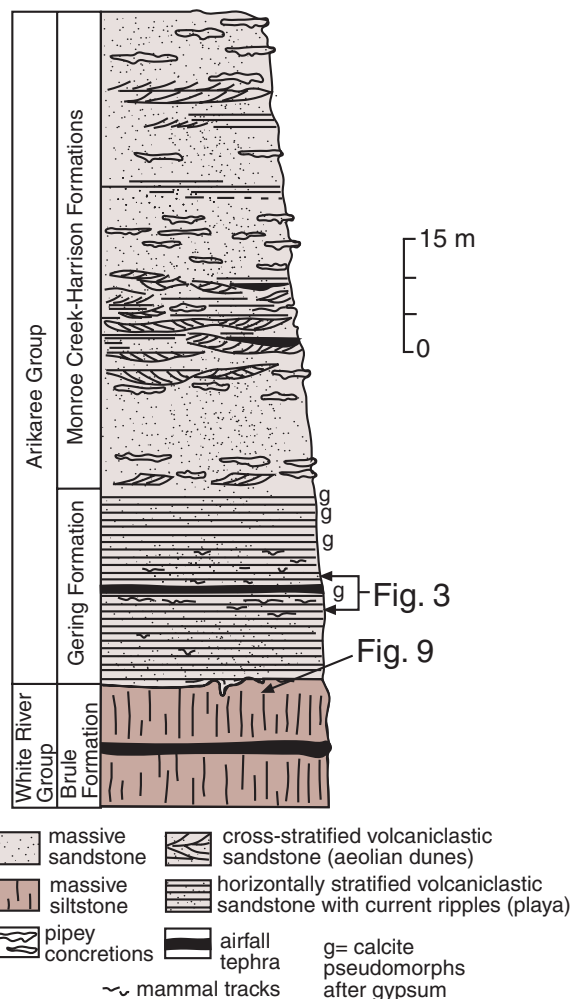


**Fig. 2.** Strata exposed at Scotts Bluff, Nebraska (modified from Swinehart & Loope, 1987).

playa may have originated via wind erosion of the land surface represented by the unconformable Brule-Gering contact (Fig. 2).

### Age and possible source of tephra and sulphur

Although Oligocene volcanism in the western United States generated an immense volume of tephra, the specific source for the ash and the sulphur within strata exposed at Scotts Bluff has not yet been identified. The Scotts Bluff tephra bed has not been isotopically dated; an earlier attempt was unsuccessful due to a lack of sanidine. Magnetostratigraphic studies of the Gering Formation at Scotts Bluff, however, place the ash bed described here within a reversed zone at the base of Chron 9, suggesting deposition took place within a time interval of about 300 000 years that ended at about 28 Ma (see Fig. 7 in Tedford *et al.*, 1996). On the basis of characteristic mineral suites, geochemistry, grain-size and Ar/Ar ages, Larson & Evanoff

(1998) concluded that the fine-grained volcanoclastics of the underlying White River Group were erupted at 35.5–30 Ma from the Great Basin of western Utah and eastern Nevada where at least 30 major, caldera-related events have been recognized (Best *et al.*, 1989). Although the volcanic glass in the Arikaree Group is sand-size (~100 microns) rather than the silt-size (~40 microns) of the older Brule Formation (Swinehart *et al.*, 1985), the samples examined from the Gering Formation contain (like the Brule) abundant hornblende, little pyroxene, and little sanidine.

The most proximal candidate for the tephra within the Gering Formation at Scotts Bluff is the San Juan Volcanic Field of south-western Colorado. With an estimated volume of 5000 km<sup>3</sup>, the Fish Canyon Tuff (28 Ma) arguably records the Earth's largest known volcanic eruption (Bachman *et al.*, 2002). It is the only unit within the San Juan Volcanic Field that contains hornblende and lacks pyroxene (Lipman, 1975), a phenocryst assemblage consistent with the tephra described here. Although silicic magmas are considered to contain relatively small amounts of dissolved sulphur, eruptions in the San Juans are thought to have released large amounts of sulphur to the atmosphere. Phenocrysts in the Huerto Formation (which immediately postdates the Fish Canyon Tuff) contain inclusions of anhydrite and pyrrhotite (Parat *et al.*, 2002). The acid-sulphate alteration in the Summitville precious metal deposit provides additional evidence of sulphur-rich magmatic vapour (Stoffregen, 1987). The Fish Canyon Tuff has normal remnant magnetic polarity (Lipman, 1975), however, and cannot be the source of the tephra in the Gering Formation unless there exists an unrecognized short-term reversal in Chron 9.

## METHODS

Grain-size analyses were made by laser diffraction, using a Coulter LS100Q instrument. Sandstone porosity was measured on photomicrographs with Object-Image (software available from the National Institute of Health). The content of clay (< 2 µm) was determined using the pipette method (Gee & Bauder, 1986), because smectite can disperse into particles too fine to be measured by laser diffraction (the lower limit of measurement by the LS100Q instrument is 0.04 µm). The extent of cementation specifically attributable to clay bonds between sand grains was evaluated, using laser diffraction particle size

analysis, after (a) soaking in deionized water; (b) shaking with sodium metaphosphate solution; or (c) soaking in 10% HCl. Deionized water is relatively ineffective in dispersing smectite and other clay mineral particles. Sodium metaphosphate effectively disperses clay minerals (Gee & Bauder, 1986), breaking down clay bonds between sand grains, but does not affect other cementing agents such as calcite. Treatment with 10% HCl destroys carbonate cementation but does not disperse clays.

## DEPOSITIONAL FACIES

### Airfall tephra

#### *Description*

This material is present in the lower Arikaree in stratigraphic units up to 1 m thick (Swinehart & Loope, 1987; Tedford *et al.*, 1996; Figs 3 and 4). The thickest tephra-rich unit is an amalgamation of at least two distinct tephra beds (Fig. 3). This facies lacks primary sedimentary structures and is typically nearly white on outcrop (Fig. 4). In thin section, it is seen to be texturally bimodal: bubble-wall shards, pumice fragments, and crystals of quartz, feldspar, hornblende and mica averaging 100 microns in diameter lie within a dense, much finer grained, glassy matrix (Fig. 5A). Grain-size analysis confirms that the particle size distribution is bimodal (Fig. 6). Lensoid pseudomorphs filled by calcite spar occur throughout this material (these and other postdepositional features associated with the tephra beds are discussed below).

### Interpretation

The texture of the material examined in thin section and SEM suggests that individual, coarse particles of glass and crystals (100 microns), fell at the same velocity as larger-diameter, less dense aggregates of much finer-grained material. These aggregates were the source of the intergranular matrix. This interpretation is consistent with observations made on modern ash falls, in which aggregation results in a bimodal particle size distribution (Carey & Sigurdsson, 1982; Rose *et al.*, 2001). Rose *et al.* (2003) have recently suggested that aggregation must also be invoked to explain the distribution of some unimodal tephtras. Their study of Miocene ash beds on the Great Plains indicates that, as the result of the extremely high surface area of individual particles, many pyroclasts would have been transpor-

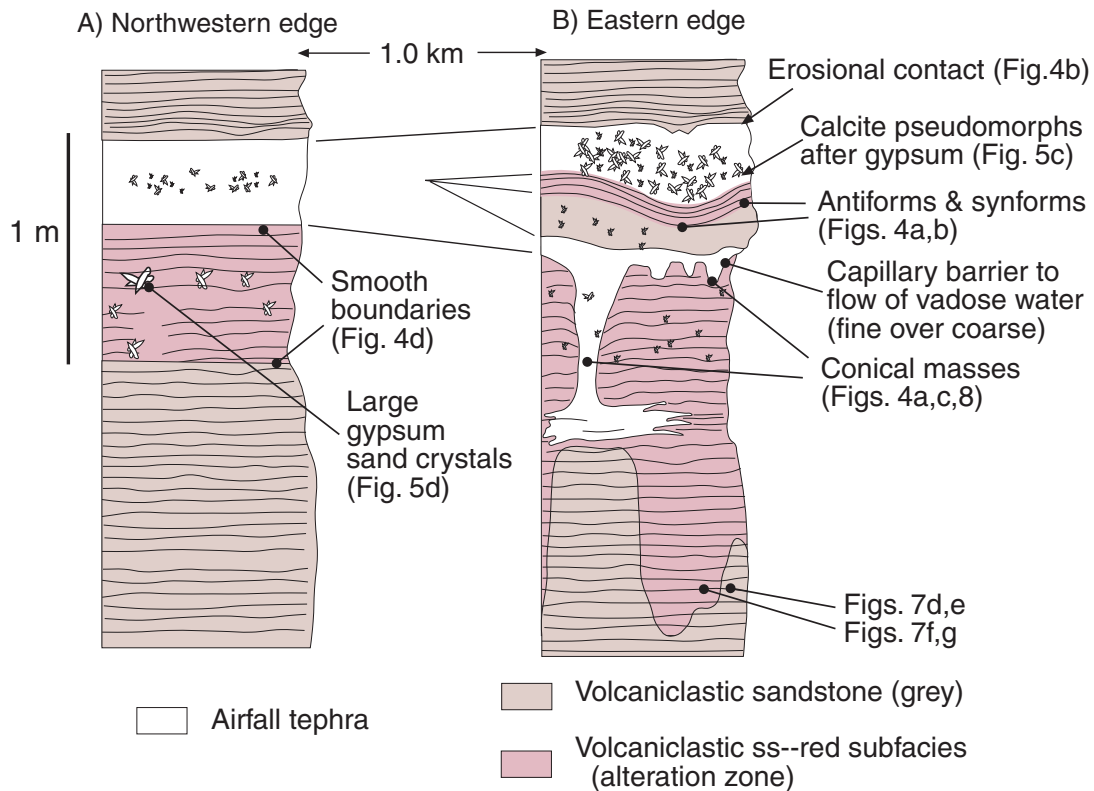


**Fig. 3.** Stratigraphic sections showing depositional facies and lateral variations in alteration zone and deformation structures. Along the north-western edge of Scotts Bluff (A), synforms, antiforms, and conical masses are absent and the alteration zone (red subfacies of volcaniclastic sandstone) is thin with a smooth lower boundary. At the eastern edge of the butte (B), the deformation structures are well-developed, and the alteration zone is thick with a highly irregular lower boundary. The irregular base of the alteration zone is interpreted as a result of preferential flow within the vadose zone, and the deformation structures as products of the displacive growth of gypsum. See Fig. 1 for locations.

ted another 1000 km further downwind if not for aggregation. Although airfall tephra commonly is laminated, the absence of primary sedimentary structures in the Scotts Bluff tephra is attributable to displacive growth of evaporite crystals (see *Early Authigenic Minerals and Their Alteration*).

### Volcaniclastic sandstone

#### Description

This material makes up more than 99% of the Gering Formation at Scotts Bluff National Monument. Sandstones are dominated by very fine sand and lack the fine matrix present in the airfall tephra. In thin section, the good sorting and the high intergranular porosity (35–50%) of these rocks clearly differentiate them from the airfall tephra (compare Fig. 5A and B). The sandstones contain abundant small-scale cross-laminae produced by migrating current (subaqueous) ripples (Fig. 4B). Delicate rhizoliths (lithified plant roots) about 1 mm in diameter are present, but are widely spaced.

#### Interpretation

The sandstones were produced through extensive wind reworking of tephra and epiclastic material, followed by local transport by runoff and subaqueous deposition on the surface of a playa. Assuming that the original airfall material had a bimodal grain size distribution, the finer mode was removed by winnowing during aeolian transport, and carried far downwind as suspended dust. All sedimentary structures in the Gering Formation within the study area indicate that the final phase of transport was subaqueous. Although no aeolian cross-strata are present in the Gering at Scotts Bluff, large-scale aeolian cross-strata are abundant in correlative rocks at nearby localities in eastern Wyoming (Bart, 1977), and in the overlying Monroe Creek-Harrison strata at Scotts Bluff (Fig. 2; Swinehart & Loope, 1987). The uniform and relatively fine grain size of the sandstone and the absence of large-scale, subaqueous cross-strata are inconsistent with deposition by a large-scale fluvial system. The abundance of primary sedimentary structures



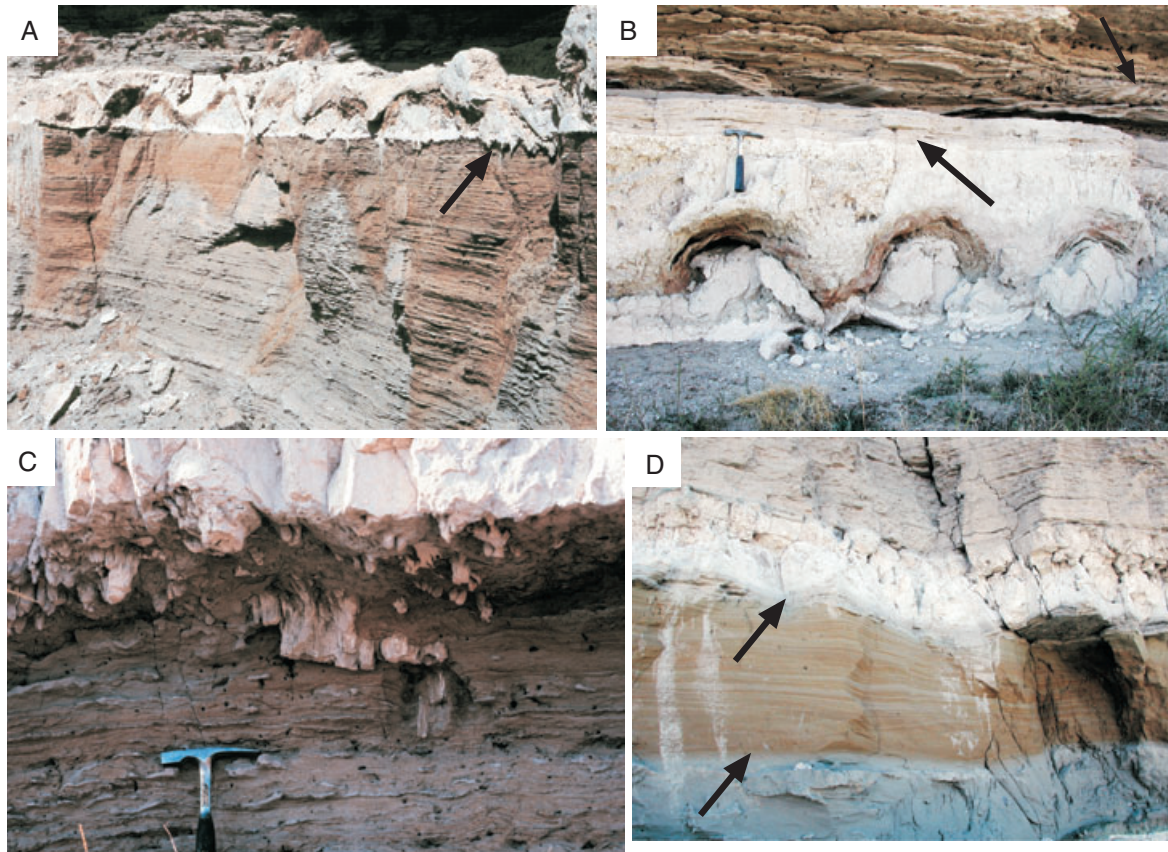


**Fig. 4.** Outcrops of alteration zone and deformation structures. (A) Antiformal and synformal structures are restricted to the white tephra zone; arrow points to conical masses projecting into reddened zone. Note irregular boundary between reddened and underlying grey (unaltered) zone, eastern edge of Scotts Bluff (Fig. 1). (B) Close-up of antiformal and synformal structures and erosive contact (lower arrow) at top of tephra. Note subaqueous climbing ripple deposits (upper arrow). (C) Conical masses projecting from base of tephra. (D) Smooth contact (upper arrow) at base of tephra (no conical masses); smooth base of red subfacies (alteration zone) marked by lower arrow. North-west edge of Scotts Bluff (see Fig. 1).

suggests that vertical aggradation was relatively continuous, without prolonged intervals of non-deposition accompanied by bioturbation and pedogenesis.

## EARLY AUTHIGENIC MINERALS AND THEIR ALTERATION

### Description

#### *Gypsum*

Calcite pseudomorphs after gypsum are abundant in the thick tephra bed and within the volcanoclastic sandstone at four stratigraphic levels (Fig. 2). Those within the tephra displaced fine-grained matrix and are now filled by calcite (Fig. 5C). Those within the sandstones grew poikilotopically, enclosing abundant sand grains, and are now represented by sand crystals cemen-

ted by calcite (Loope, 1986; Swinehart & Loope, 1987; Fig. 5C). Samples from the latter type of pseudomorph, collected near the north-west edge of Scotts Bluff just below the tephra, revealed the strongest  $^{17}\text{O}$  anomaly reported by Bao *et al.* (2000) and Bao *et al.* (2003).

In the field, calcite pseudomorphs after gypsum appear to be most abundant in the upper 20–30 cm of the tephra zone, where the calcite content is 75–80% of the rock mass (measured by the Chittick method; Machette, 1985). Samples with few pseudomorphs have much less calcite (1–10%), indicating that nearly all calcite occurs as pseudomorphs.

#### *Smectite and zeolite*

Smectite coatings are present on the surfaces of glass particles. These coatings have a reticulate or 'honeycomb' fabric in which clay platelets lie perpendicular to the surfaces of the clasts and on

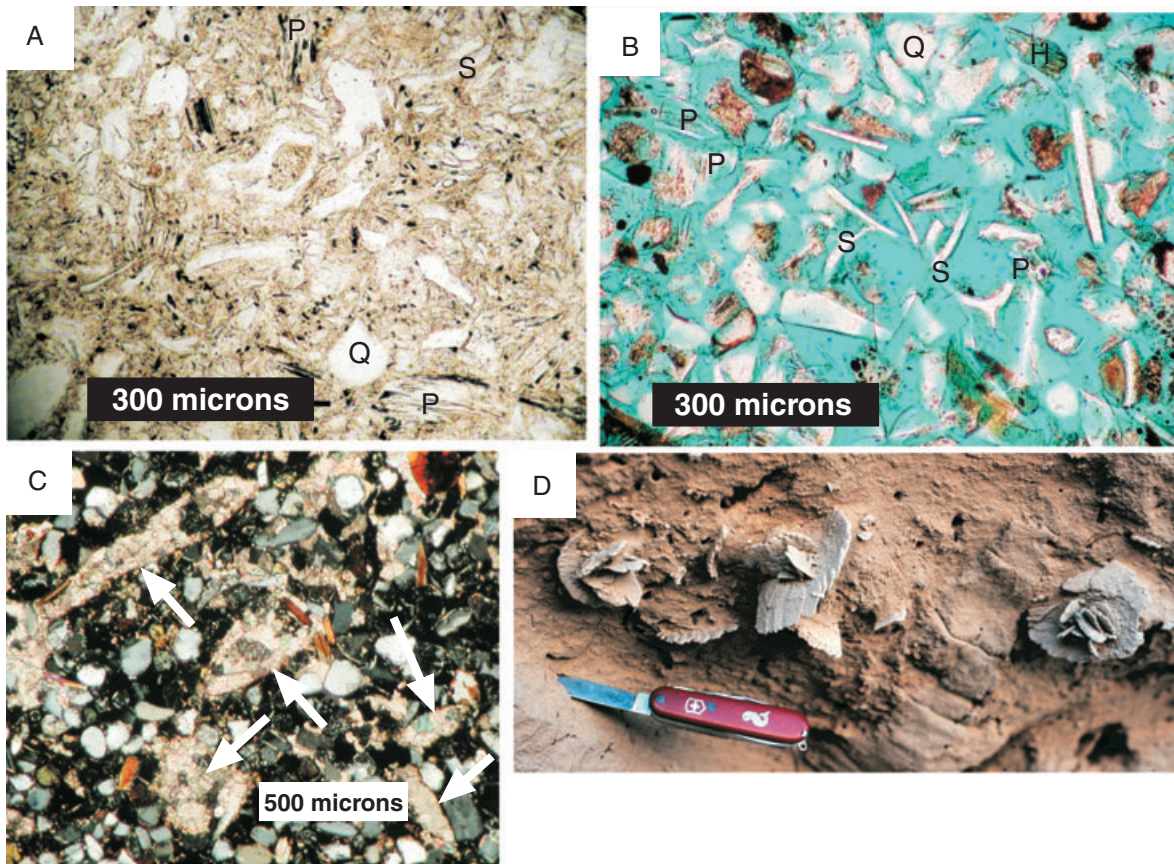


**Fig. 5.** (A) Photomicrograph of airfall tephra (plane light). Note bimodal texture with sand-size clasts in a finer-grained, brownish matrix; (B) reworked volcaniclastic sandstone (plane light; dark material between well-sorted grains is blue epoxy). Note abundant bubble-wall glass shards (S), pumice (P), and quartz (Q) in both (A) and (B), and hornblende (H) in (B). (C) Calcite-filled pseudomorphs after lensoid gypsum (arrows) within volcaniclastic sandstone; (D) pseudomorphs of gypsum sand crystals, now cemented by calcite. Knife handle is 9 cm long.

vesicle walls (Fig. 7A–C; Stanley & Benson, 1979; Schenk, 1990). Examination with SEM also reveals the presence of tabular crystals of clinoptilolite (zeolite group, Fig. 7C), and external molds of vesicles (Fig. 7B).

#### *Alteration zone*

An alteration zone marked by a red subfacies of the volcaniclastic sandstone is found immediately below, or interbedded with, the airfall tephra (Figs 3 and 4). This rock is more friable than the unaltered volcaniclastic sandstone and forms a weak zone within the cliff-forming Arikaree Group at Scotts Bluff; cliff retreat commonly occurs through failure of slabs based within the red subfacies. Along the eastern edge of Scotts Bluff, the irregular base of this reddened sandstone crosscuts bedding, and displays as much as 3 m of relief over horizontal distances of <5 m (Figs 3 and 4A). This irregular surface can be traced along the full length of a 30 m long

tunnel, demonstrating that the alteration zone is not a surficial feature. At the north-west edge of Scotts Bluff, the base of the reddened zone is smooth and nearly parallel to bedding, and the base of the thick tephra bed lacks conical projections (Figs 3 and 4D). Within the red subfacies, calcite-spar-filled pseudomorphs after gypsum are locally present, and large calcite-cemented masses of sandstone that represent former gypsum sand crystals (Loope, 1986) are present in exposures along the north-west face of Scotts Bluff (Fig. 5D). Smaller gypsum sand crystal pseudomorphs are also present within the grey (unaltered) sandstone above the tephra (Fig. 2). Analysis of calcareous tephra and sandstone samples after treatment with 0.1 M HCl indicates that the sulphate content of calcite is extremely high and variable, ranging from about 2000 p.p.m. to about 38 000 p.p.m. The highest value is from calcite pseudomorphs after gypsum in the upper part of the thick tephra.



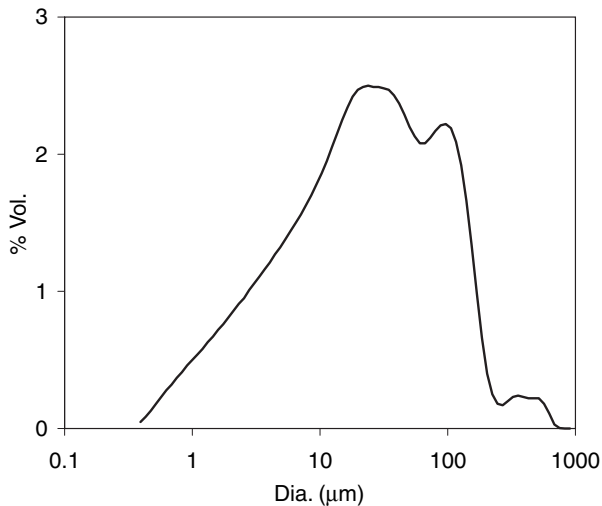


**Fig. 6.** Particle size distribution of airfall tephra, sampled near base of tephra zone. Sample was sonicated for 15 min before analysis in Coulter LS100Q particle sizer. Peak at about 25 microns represents glassy matrix; peak at about 100 microns represents population of larger shards, pumice and crystals. Minor peak around 400 microns represents residual aggregates of fine glass particles. These could be the original airfall aggregates, but are more likely to be fragments of the lightly cemented sediment that were not completely disrupted by sonication.

Three pairs of samples were collected from the altered and unaltered rocks along individual bedding planes crossed by the 'alteration front' at the base of the red subfacies (Fig. 3). Under the SEM, each sample of the grey, unaltered material displays pervasive smectite grain coatings and bridges between grains (Figs 7D and E), with a 'honeycomb' fabric similar to that observed in the airfall tephra. Each sample from the red subfacies displays only vestiges of 'honeycomb' fabric (Figs 7F and G). Although the smectite coatings are visually prominent in the unaltered material, they are a very small fraction of total rock mass. Both altered and unaltered sandstones contain < 2% clay. The measured clay content of each unaltered sample was 1.5–2 times that of its paired red subfacies sample, but the difference is not significant relative to typical measurement error.

### Interpretation

The airfall tephra was modified to varying degrees by formation of authigenic smectite, zeolites and gypsum (subsequently replaced by calcite). Smectite and zeolites are the most common weathering products of volcanic glass in contact with alkaline

pore waters (Fisher & Schminke, 1984). Alkaline conditions are to be expected when the products of hydrolysis reactions between rainwater and igneous rock are concentrated by evaporation (Garrels & McKenzie, 1967; Hardie & Eugster, 1970). Whereas smectite can form at a wide range of pH values, in a variety of settings including the unsaturated zone, the presence of clinoptilolite strongly suggests a saline/alkaline lake environment. A likely analogue would be alkaline playas such as those common today on the High Plains. Occasional contact with alkaline waters in a playa would result in some dissolution of glass (indicated by the external molds of vesicles) and formation of limited quantities of zeolites, but not the more extensive zeolitization of glass that occurs in sediments of perennial saline lakes (Fisher & Schminke, 1984; Lander & Hay, 1993).

### Gypsum

The presence of calcite pseudomorphs after gypsum indicates evaporative concentration beneath the playa surface. Gypsum precipitation could have occurred in a groundwater-discharging playa. Alternatively, the playa could have been fed by rainfall and surface runoff water ponded for short intervals above a thick vadose zone; gypsum precipitation within the shallow vadose zone is common in arid or semiarid environments (Watson, 1983). Alteration and deformation features, discussed below, suggest that the playa waters were in fact perched above a vadose zone at least several metres thick.

Crystallization of copious gypsum within these strata requires not only the concentration of pore waters by evaporation, but also requires a significant influx of sulphate. Previous work on stable oxygen and sulphur isotopes by Bao *et al.* (2000, 2003) has identified sulphate aerosols as the primary source of this sulphate. Anomalous  $^{17}\text{O}$  values in sulphate extracted from the airfall tephra indicate atmospheric oxidation of sulphur gases by ozone or hydrogen peroxide. Sulphur isotope ratios near zero or slightly positive are consistent with a volcanic origin, and are inconsistent with derivation from groundwater from the Pierre Shale.

### Estimation of the mass of precipitated sulphate

The mass of gypsum formerly present per square metre of the upper surface of the tephra can be calculated using the estimated mass fraction of calcite (assumed to occur almost entirely within pseudomorphs), measured bulk densities of samples from the tephra range ( $1.4\text{--}1.6\text{ g cm}^{-3}$ ), and



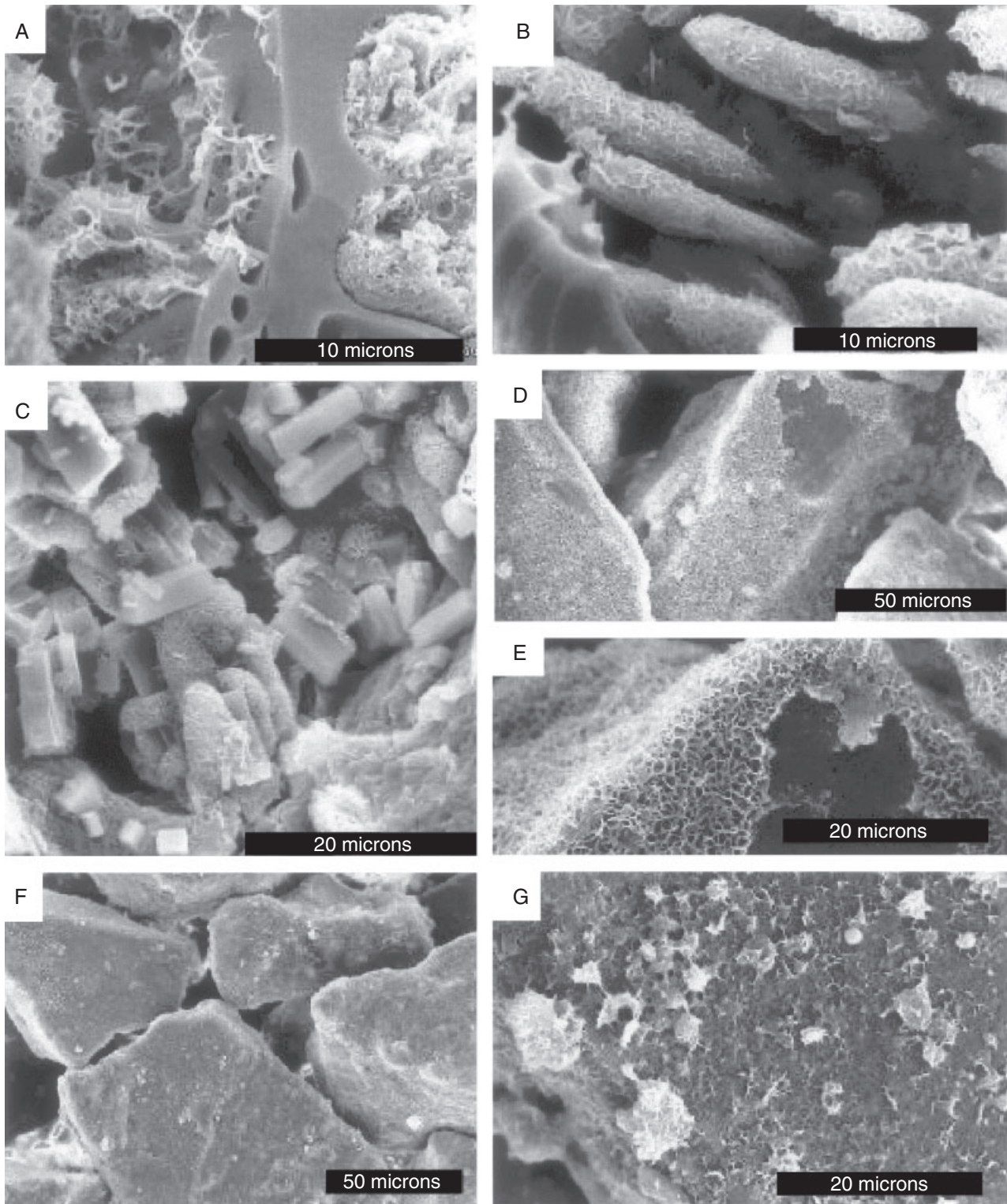


**Fig. 7.** SEM images from airfall tephra (A–C); volcanoclastic sandstone (D and E); and the red subfacies of volcanoclastic sandstone (F and G). (A) Glass shard with authigenic smectite coatings. (B) External molds of vesicles that were coated with smectite before dissolution of parent glass shard. Dissolution is interpreted as having taken place under strongly alkaline conditions. (C) Tabular crystals of clinoptilolite – a zeolite mineral indicative of alkaline conditions. (D and E) Reticulate ('honeycomb') smectite coatings on well-sorted sand grains. Coatings have broken away from grain surfaces at former points of grain contact. (F and G) Sand grains from same stratum as previous images, but within altered zone (red subfacies), where vestiges of smectite cement reflect dissolution by descending, acidic pore waters (see Fig. 3B).

typical particle densities for calcite ( $2.7 \text{ g cm}^{-3}$ ) and gypsum ( $2.3 \text{ g cm}^{-3}$ ). Only the particularly abundant calcite pseudomorphs after gypsum in the uppermost 20–30 cm of the tephra are considered; volumetric content of pseudomorphs in the underlying strata is highly variable, but generally much less. Given a minimum calcite mass fraction of 0.75, the calcite now present in the upper 20 cm of the tephra replaced about 180–200 kg of gypsum per square metre of the upper surface of the tephra. If all of that gypsum originated as sulphate aerosol deposited directly on the playa surface from dry fogs or directly associated with volcanic ash, it would represent sulphate deposition rates  $> 100 \text{ kg m}^{-2}$  ( $10^8 \text{ kg km}^{-2}$ ). It is possible that some of the sulphate precipitated in the small playa was derived from non-volcanic sources, but this would only increase the amount of sulphate aerosol required to generate the high isotopic anomaly reported by Bao *et al.* (2000, 2003). The precipitated gypsum was derived from volcanic sulphate deposited not only on the playa itself, but also in the surrounding catchment, from which it was reworked by slope wash. Furthermore, the sections displaying abundant pseudomorphs in the tephra may represent deeper parts of the playa, in which sulphate was concentrated as the shallower parts were desiccated. Assuming that these processes locally concentrated sulphate by a factor of 1000, then the average rate of sulphuric acid deposition across the playa and its catchment could still have exceeded  $100\,000 \text{ kg km}^{-2}$ . For comparison, Thordarson & Self (2003) estimate that sulphuric acid deposition from Laki was about  $1000 \text{ kg km}^{-2}$ , averaged over the Northern Hemisphere north of  $30^\circ\text{N}$ . Those authors noted that deposition was actually concentrated in western Europe, where it probably occurred at ‘many times’ the zonal average of  $1000 \text{ kg km}^{-2}$ .

Although the calcite pseudomorphs after gypsum in the uppermost tephra potentially represent  $> 100 \text{ kg m}^{-2}$  of  $\text{H}_2\text{SO}_4$ , much of this may have been neutralized in the atmosphere before deposition. Historical records of the Laki eruption (Grattan & Pyatt, 1994) show that distal fallout can be strongly acidic, but sulphuric acid can also be neutralized before deposition through reaction with mineral grains or glass shards. Neutralization is particularly likely for acid carried into the playa by slope wash. However, even a small fraction of this potential acidity mixed with infiltrating waters could yield very low pH values in the underlying reworked sandstone. During the intervals between major eruptions, rainfall,

weathering of volcanic glass and evaporation from the playa surface produced waters that precipitated calcite, smectite, and clinoptilolite, and became increasingly alkaline and calcium-poor. The sulphate delivered to the playa in the wake of distant eruptions dissolved some of these precipitates. Following concentration by evaporation, copious gypsum precipitated in the sediment just below the surface of the playa.

#### *Smectite*

Despite the very low clay content in both the tephra and the volcanoclastic sandstones, particle size analyses using various pretreatments (see *Methods*) indicate that smectite plays a critical role in cementing the sandstones. Loss of part of this smectite from the red subfacies has made it significantly more friable. Red subfacies samples display very similar particle size distributions when soaked in deionized water or treated with sodium metaphosphate solution; this indicates weak, readily broken clay bonds between sand grains. In contrast, grey sandstone samples display a distinctly finer particle size distribution after sodium metaphosphate treatment than in deionized water alone, indicating that clay bonds were stronger in these rocks and held together residual aggregates of sand grains following the deionized water treatment. Treatment with 10% HCl does not affect dispersion of either rock type, ruling out significant carbonate cementation outside the pseudomorphs.

Following Stanley & Benson (1979), the reticulate smectite is here interpreted as an early cement formed as a weathering product. Similar authigenic smectite is common throughout much of the Arikaree and White River groups, including strata in which sedimentary structures are well preserved. This distribution indicates that formation of the smectite did not require intense weathering or pedogenesis, and probably occurred in a variety of environments including the vadose zone.

The abundance of reworked volcanic material relative to airfall tephra, in the Gering Formation at Scotts Bluff and in the Arikaree Group as a whole, indicates that the reworking process was highly efficient. Nonetheless, the Gering sandstone at Scotts Bluff represents relatively rapid vertical accretion of sand on a playa surface that was likely to have been exposed to high winds and high rates of evaporation. This may be explained by early, light cementation provided by authigenic smectite. Rapid cementation below a temporary, perched water table would have retarded aeolian deflation, and ultimately allowed

vertical accretion after numerous episodes of reworking of airfall particles. The rare preservation of airfall material probably took place only close to the playa centre where interstitial water and gypsum cements prevented deflation.

#### *Smectite alteration*

The vestiges of 'honeycomb' smectite seen in SEM images (Fig. 7F and G) suggest that grain-coating clays were once pervasive on sand grains of the red subfacies, but were largely removed, weakening the red subfacies relative to the grey (unaltered) volcanoclastic sandstone. The removal of smectite from bedded sandstone of the red subfacies would require either dissolution or dispersion and eluviation of clay particles to deeper horizons. There is no evidence of redeposited clay at the base of the red subfacies or deeper in the Gering sandstone; therefore, it is inferred that the smectite was removed by dissolution. The colour of the red subfacies can be explained through precipitation of iron oxides after the Fe-bearing smectite was dissolved. This dissolution did not occur during long-term weathering in a palaeosol: the preservation of primary stratification, with only widely scattered, thin rhizoliths is inconsistent with a prolonged interval of non-deposition and pedogenesis. In any case, smectite can apparently persist over long periods of time in some acidic (pH 4–5) soils (e.g. Karathanasis *et al.*, 1986; Mason *et al.*, 1994).

The highly irregular lower boundary of the red subfacies that is often discordant to bedding along the eastern edge of Scotts Bluff (Figs 3B and 4A), provides important additional insight: alteration most likely occurred as ponded water near the playa centre infiltrated into unsaturated sediment behind an irregular wetting front. Soil physicists increasingly recognize that irregular wetting fronts, with infiltrating water advancing much more rapidly in some locations than others, are very common, particularly where fine-grained material (the airfall sandy siltstone) overlies coarser-grained sediment (the reworked sandstone) (Stephens, 1996). Where the lower boundary of the red facies is smooth (along the north-west edge of Scotts Bluff; Fig. 4D), lateral flow of groundwater, and a slightly higher position on the playa floor are inferred. The restriction of large gypsum sand crystals to this inferred position may reflect slower crystal growth from more dilute pore waters.

Calcite-spar-cemented, pipe-like concretions are abundant in conformable strata that lie directly above the Gering Formation (Fig. 2). These concretions maintain a consistent north-

east-south-west orientation over much of the southern Nebraska panhandle, and are interpreted as products of early cementation in the phreatic zone (Swinehart & Loope, 1987). Within the lensoid calcite pseudomorphs after gypsum (Fig. 5C), the highly variable sulphate content (up to 38 000 p.p.m. with respect to CaCO<sub>3</sub>) probably reflects preservation of small gypsum inclusions. Like the cement in the pipe-like concretions, these coarse calcite crystals also grew under phreatic conditions that prevailed as the water table rose through the accumulating sediment.

## DEFORMATION STRUCTURES

### Description

#### *Small folds*

Antiforms and synforms with wavelengths of 0.5–2 m and amplitudes of about 60 cm are developed in the sediments immediately below the erosional surface at the top of the tephra (Figs 3B, 4A and B). The synforms are the sites with the greatest abundance of calcite pseudomorphs after gypsum. At the crests of antiforms, the tephra is commonly truncated by erosion and is directly overlain by undeformed beds of the volcanoclastic sandstone facies.

#### *Conical masses*

Cones of airfall tephra ranging from a few cm to over a metre in length project from the base of the tephra (Fig. 4A and C). Down-warped laminae in the altered (red) sandstone are present directly below the tips of the projections (Fig. 8)

#### *Irregular, large-scale convolutions*

Convolutions with amplitudes of at least 2 m and a wavelength of about 3 m are present 10 m below the tephra at the unconformable contact between volcanoclastic sandstones of the Gering Formation and the volcanoclastic siltstones of the underlying Brule Formation (Figs 2 and 9). The convolutions affect only the basal 1–2 m of the Gering sandstone; bedding above that deformed zone is flat.

### Interpretation

#### *Small folds*

These structures are interpreted as byproducts of displacive evaporite growth (Fig. 10). Enterolithic folds generated by displacive evaporite growth have been illustrated from the walls of trenches dug in many modern sabkhas and playas. Lateral



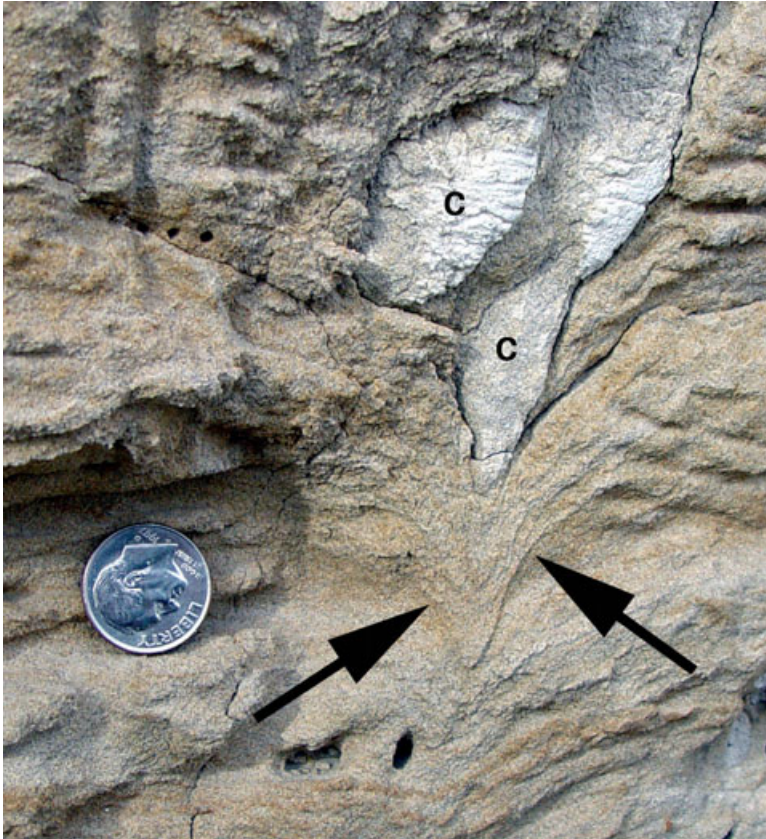


**Fig. 8.** Deformation of laminae within red subsol (altered zone) beneath a conical mass of tephra (c) that projects downward from the overlying bed. As gypsum grew displacively in higher strata, tephra was forced down ‘fingers’ of water-saturated sediment that developed along the capillary barrier to vadose flow at the base of the tephra bed. The sand surrounding the conical masses remained dry and resisted deformation (see Fig. 10). Diameter of coin is 1.8 cm.

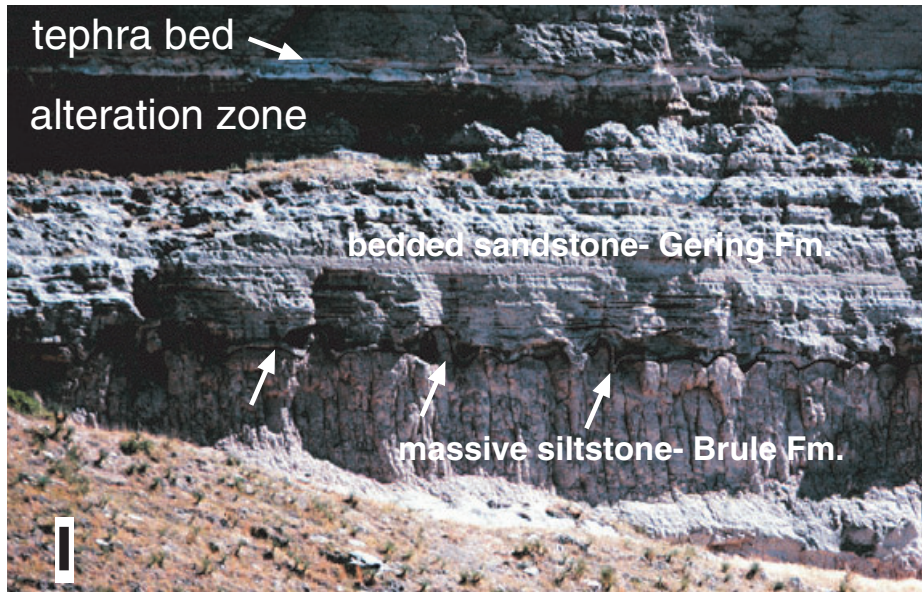


**Fig. 9.** Soft-sediment deformation along the contact (arrows) between the Brule and Gering Formations. Black scale bar represents 2 m. Deformation is interpreted as a case of loess collapse: high porosity, low permeability aeolian siltstone of the Brule Formation had not been saturated by water until after burial by sandstones of the basal Gering Formation. Note vertical joints in uppermost Brule Formation. The sandstones represent the initial fill of a small playa. Vertical movement of water through the basal sands from the playa centre led to saturation and collapse of siltstone.

and vertical forces generate broadly similar structures in the unconsolidated materials within the active zone above permafrost (Washburn, 1973)

and within vertic soils (Wilding & Tessier, 1988). Following Warren (1989; p. 50), who called attention to the interplay of displacive evaporite



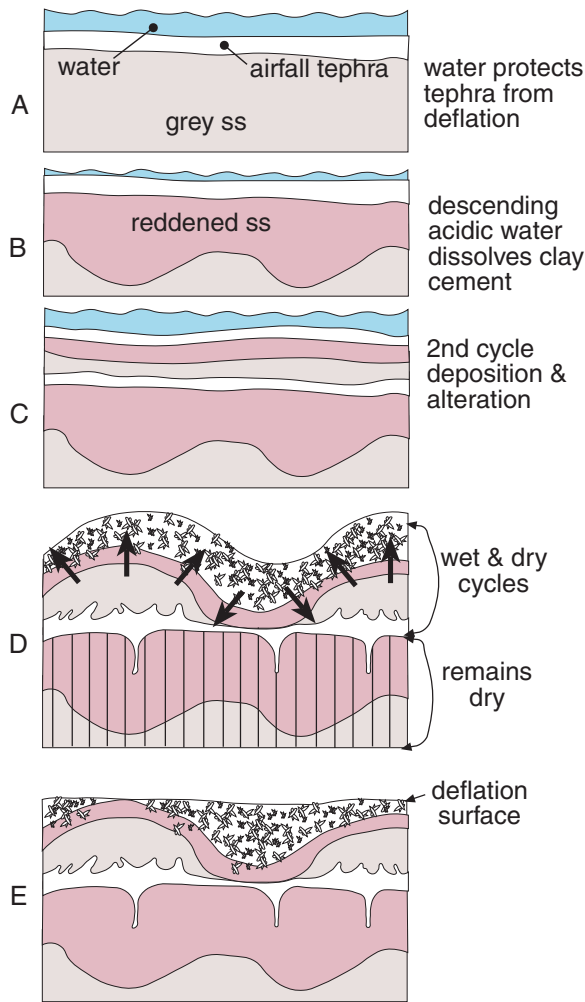


**Fig. 10.** Interpreted sequence of events during development of alteration zones and deformation structures at the playa centre. (A) Tephra deposited on wet surface of alkaline playa with deep water table. (B) Lower alteration zone develops as ponded, low-pH water percolates downward, dissolving smectite cement of underlying grey ss. (C) Fluvial deposition of volcanoclastic sand on lower tephra, followed by renewed deposition of tephra and development of upper alteration zone. (D) Evaporation of sulphate-rich water leads to displacive growth of gypsum in the upper tephra, and to buckling of strata. Sediment below lower tephra remains dry (and resistant) except in 'fingers' of preferential flow of pore water. Tephra is pushed downward, displacing the weak sediment in the water-saturated 'fingers' and forms conical masses. Note that conical masses are: (1) restricted to the altered zone (where smectite cement was previously removed by acidic pore water) and (2) were localized by the capillary barrier formed where the tephra (with a fine-grained matrix) overlies grain-supported volcanoclastic sandstone. (E) Deflation of playa surface removes crests of antiforms.

growth and aeolian deflation on sabkha surfaces, the surface that truncates the antiforms is interpreted as being a result of deflation.

### Conical masses

The distinct morphology, broad range of diameters, and close spacing of the masses are inconsistent with an origin as passive fills of burrows. Although the roots of vascular plants can take a similar form, the preserved bedding directly adjacent to the cones makes a root origin highly unlikely. The deformed laminae below the tips of the cones instead attest to an origin from downward injection. Where sands (high density) overlie unconsolidated muds (low density), bulbous masses of sand can sink into the mud to form load casts or 'ball and pillow' structures. These structures are formed by buoyant forces while the sediments are in a liquified state (Allen, 1970; p.86). In the present case, neither the morphology of the projections, nor the stratigraphy is consistent with this mechanism.

In unstable flow of vadose water, downward propagation of the wetting front proceeds as discrete fingers instead of as a uniform plane (Hillel, 1980; Stephens, 1996). Where the water table lies far below the surface and fine-grained surficial sediment lies above well-sorted sand, the upper material must become nearly completely water-saturated before the water 'breaks through' to the coarser, higher permeability material. 'Fingers' occupy only a portion of the horizontal cross-section, with air remaining in the pore spaces in the surrounding sediment. Further, the same 'fingers' of preferential flow are repeatedly occupied by vadose water during successive, subsequent infiltration events (Stephens, 1996). The conical projections at the base of the tephra are attributed to plastic deformation following the development of a capillary barrier (fine sediment over coarse) associated with the unstable flow of vadose water. As gypsum crystals grew within and displaced the overlying, water-saturated, finer-grained sediment, 'finger flow' was taking place in the underlying sand. The 'fingers' became conduits down which airfall tephra was forced, but the intervening unsaturated sand (with much greater strength than the sand within the 'fingers') was not penetrated (Figs 3 and 10). The final volume of gypsum growth and the full extent of deformation probably were accomplished only after many cycles of wetting and drying of the sediments that lay very near the playa surface.

### Irregular, large-scale convolutions

The large-scale convolutions at the Brule-Gering contact formed after deposition of the initial increment of Gering sands, but did not propagate

more than 1–2 m above the base of the Gering. Thus, this deformation predates the overlying tephra beds and cannot be clearly linked to acid deposition. These convolutions are interpreted as products of the collapse of the Brule siltstone during initial saturation, directly analogous to collapse of Quaternary loess – a phenomenon important in geotechnical engineering. The Brule Formation is widely interpreted as an aeolian deposit analogous to Quaternary loess, but with a composition dominated by silt-sized volcanic glass shards (Swinehart *et al.*, 1985). Loess collapse involves particle rearrangement from a metastable open structure to a denser, stable hydrocollapsed structure. If the Brule Formation is essentially volcanoclastic loess, deposited well above the water table, it could have retained an open structure until long after deposition. In an arid or semiarid setting, infrequent rains rarely infiltrate deeply into such fine-grained sediment. Instead, precipitation becomes runoff or wets a shallow surficial zone from which it is removed by evapotranspiration.

Conditions allowing deep wetting and collapse of the Brule Formation could have developed along with the playa basin proposed here as the setting of sandstone deposition in the Gering Formation. The playa developed over a closed depression on the upper surface of the Brule Formation, representing either depositional topography or a deflation basin. Regional stratigraphic correlations and the absence of a palaeosol at the top of the Brule Formation, however, suggest that the upper contact is an erosional disconformity. Aeolian deflation is a leading hypothesis for Quaternary playa basin formation on the Great Plains. Once the basin formed, it allowed ponding of rainfall and runoff water above the unsaturated Brule Formation. This in turn led to focused infiltration beneath the playa centre, wetting the underlying silt enough to cause it to collapse. Focused infiltration beneath present-day playas is recognized in the Southern High Plains of Texas and New Mexico, where it leads to preferential dissolution of carbonates underlying playa basins (Osterkamp & Wood, 1987).

## DISCUSSION

Interpretation of the depositional setting as a relatively small, surface-water-discharging, alkaline playa is consistent with previous work (Tedford *et al.*, 1996) and with new sedimento-

logical observations, and helps to explain the geological preservation of the isotopic signature of the sulphate. In this depositional setting, neither leaching to the regional water table, nor flooding by surface waters rich in non-anomalous sulphate removed, diluted, or prevented the detection of the anomalous sulphate. In particular, the small catchment area of the playa and the great depth to groundwater beneath its surface prevented removal and strongly reduced dilution, and the paucity of organic matter prevented sulphate bacterial fractionation of the sulphate. A small, virtually unvegetated, rarely flooded, alkaline playa that was subject to aeolian deflation and rapid desiccation would have been a strongly oxidizing setting in which organic matter was sparse and bacterial sulphate reduction minimal.

In light of the *prima facie* geochemical evidence for an atmospheric source of the sulphates collected from these rocks (Bao *et al.*, 2003), it is inferred that smectite dissolution was accomplished within a short interval by infiltration of very low pH meteoric water derived from dry fogs and by leaching of sulphuric acid from the airfall tephra. If enough sulphuric acid was mixed with rainfall and runoff water in the playa, and then infiltrated into underlying unsaturated sands, the pore water wetting those sands could have reached much lower pH values than those observed in most acidic soils. This in turn would allow rapid smectite dissolution. Laboratory studies indicate that the rate of smectite dissolution increases by more than two orders of magnitude between pH 7 and pH 1 (Huertas *et al.*, 2001). Using the relation between pH and dissolution rate proposed by Huertas *et al.* (2001), the half-life of smectite is a little more than 2 yr at pH 2 and slightly less than 1 yr at pH 1. Laboratory studies may exaggerate rates of dissolution in the field, but these studies do suggest that extreme acidification, to pH 2 or less, could result in rapid dissolution of a small, but critically important mass of smectite, converting the grey volcanoclastic sandstone into the more friable red subfacies. Under the field conditions considered here, especially rapid dissolution of the 'honeycomb' smectite coatings would be favoured by their extremely high surface area to mass ratio and their location adjacent to large pores between sand grains.

The abundant calcite pseudomorphs after gypsum in the airfall tephra provide key evidence that such dramatic acidification is plausible. Evidence for a volcanic origin of sulphate

contained in these pseudomorphs, presumed to be inherited from the original gypsum, is described above. The mass of gypsum represented by the pseudomorphs provides an estimate of the quantity of volcanic sulphate that could have been present in pore waters beneath the playa floor around the time the tephra was deposited. This would include much of any sulphate that was carried downward into the altered zone (red subfacies) by infiltrating playa waters. When the playa itself subsequently dried up, evaporation from the exposed playa floor would create a strong gradient driving unsaturated flow of water upward from underlying sediment, transporting sulphate back into the tephra.

The presence of gypsum sand crystal pseudomorphs within grey volcanoclastic sandstones that lie above the tephra (Fig. 2) indicates that evaporative concentration of pore waters to gypsum saturation took place many times during deposition of the Gering Formation. Although acid deposition may have been a common event, on only one occasion was enough acid delivered to sufficiently alter the initially high-pH pore water composition to dissolve the smectite coatings and redden the subsurface sand. The abundant aeolian cross-strata within the Arikaree Group (Bart, 1977) indicate that, during the late Oligocene, the Great Plains was sparsely vegetated and swept by westerly winds. Watson (1983) notes that in arid and semiarid settings, gypsum crusts frequently protect underlying sediments from erosion. At the Scotts Bluff playa, wetting of the fine-grained tephra that bears the isotopic anomaly would have made it cohesive, and interstitial growth of abundant, sand-free gypsum crystals would have made it even less vulnerable to deflation.

The only eruptions observed to generate dry fogs have been basaltic; such eruptions release about 10 times more sulphur than equal volumes of silicic magma (Devine *et al.*, 1984). The only geochemical signature within ancient strata that has been attributed to an ancient dry fog event, however, is from a silicic tephra. The isotopic anomaly at Scotts Bluff could record widespread tropospheric pollution generated by a silicic super-eruption. Because no such eruptions have been witnessed, knowledge of the atmospheric loading by tephra and gas associated with super-eruptions is vague and entirely based on much smaller contemporary examples.

Alternatively, it is conceivable that the volcanogenic sulphate and the silicic tephra came from different sources. In this scenario, the tephra bed

hosts the anomaly only because its fine-grained matrix played a crucial role in preserving the sulphate within the otherwise sand-dominated playa deposits.

## CONCLUSIONS

1. Tephra beds and reworked tephra in under- and overlying strata accumulated on the surface of a small, wind-swept playa with a deep water table.

2. Between sulphate aerosol deposition events, rainfall, the weathering of volcanic glass and evaporation from the playa surface produced waters that precipitated calcite, smectite, and clinoptilolite as they became increasingly alkaline and calcium-poor. The occasional delivery of sulphuric acid to the playa in the wake of distant eruptions dissolved some of these precipitates and formed a prominent, reddened alteration zone.

3. When dry fogs delivered copious sulphate, evaporation led to gypsum crystallization. In the playa centre, gypsum growth displaced surrounding sediment, generated large folds, and pushed conical masses of tephra into the underlying altered zone.

4. The  $^{17}\text{O}$  anomaly was preserved because the far-travelled sulphates did not mix with large quantities of surface or groundwater, and organic matter was relatively sparse in the surficial sediments of the playa. Although most gypsum was replaced by calcite, inclusions of this mineral with the original, anomaly bearing sulphate were apparently preserved.

## ACKNOWLEDGEMENTS

We thank the ranger staff at Scotts Bluff National Monument for their help and co-operation during field work. Discussions with J.B. Swinehart provided helpful insights. Reviews by C. Taberner and T. Thordarson greatly improved the paper. This project was supported by funds from the Schultz Chair in Stratigraphy at the University of Nebraska.

## REFERENCES

- Allen, J.R.L. (1970) *Physical Processes of Sedimentation*, 4th edn. Allen & Unwin, London.  
 Bachman, O., Dungan, M.A. and Lipman, P.W. (2002) The Fish Canyon magma body, San Juan volcanic field, Colorado:

- Rejuvenation and eruption of an upper-crustal batholith. *J. Petrol.* **43**, 1469–1503.
- Bao, H., Thiemens, M.H., Farquhar, J., Campbell, D.A. and Loope, D.B.** (2000) Anomalous  $^{17}\text{O}$  compositions in massive sulfate deposits on the Earth. *Nature*, **406**, 176–178.
- Bao, H., Thiemens, M.H., Loope, D.B. and Yuan, X.-L.** (2003) Sulfate oxygen-17 anomaly in a Cenozoic Oligocene ash bed in mid-North America: Was it the dry fogs? *Geophysical Research Letters*, **30**(16), 1843, doi: 10.1029/2003GL016869.
- Bart, H.A.** (1977) Sedimentology of cross-stratified sandstones in Arikaree Group, Miocene, southeastern Wyoming. *Sed. Geol.* **19**, 165–184.
- Best, M.G., Christiansen, E.H., Deino, A.L., Gromme, C.S., McKee, E.H. and Noble, D.C.** (1989) Eocene through Miocene volcanism in the Great Basin of the western United States. *New Mexico Bureau Mines Mineral Resources Memoir*, **47**, 91–133.
- Carey, S.N. and Sigurdsson, H.** (1982) Influence of particle aggregation on deposition of distal tephra from the May 18, 1980, eruption of Mount St. Helens volcano. *J. Geophys. Res.* **87**, 7061–7072.
- Devine, J.D., Sigurdsson, H. and Davis, A.N.** (1984) Estimates of sulphur and chlorine yield to the atmosphere from volcanic eruptions and potential climatic effects. *J. Geophys. Res.* **89**, 6309–6325.
- Fisher, R.V. and Schminke, H.U.** (1984) *Pyroclastic Rocks*. Springer-Verlag, Berlin.
- Garrels, R.M. and McKenzie, F.T.** (1967) Origin of the chemical compositions of some springs and lakes. Equilibrium Concepts in Natural Water Systems. *Am. Chem. Soc. Adv. Chem. Series*, **67**, 222–242.
- Gautier, D.L.** (1987) Isotopic composition of pyrite: relationship to organic matter type and iron availability in some North American Cretaceous shales. *Chem. Geol.* **65**, 293–303.
- Gee, G.W. and Bauder, J.W.** (1986) Particle size analysis. In: *Methods of Soil Analysis* (Ed. A. Klute) Part 1, pp. 383–411. Amer. Soc. Agronomy, Madison, WI.
- Grattan, J.P. and Pyatt, F.B.** (1994) Acid damage to vegetation following the Laki fissure eruption in 1783 – an historical review. *Sci. Total Environ.* **151**, 241–247.
- Hardie, L.A. and Eugster, H.P.** (1970) The evolution of closed-basin brines. *Mineral. Soc. Am. Spec. Publ.* **3**, 171–200.
- Hillel, D.** (1980) *Fundamentals of Soil Physics*. Academic Press, San Diego.
- Huertas, F.J., Caballero, E., Jimenez de Cisneros, C., Huertas, F. and Linares, J.** (2001) Kinetics of montmorillonite dissolution in granitic solutions. *Appl. Geochem.* **16**, 397–407.
- Karathanasis, A.D., Hurt, G.W. and Hajek, B.F.** (1986) Properties and classification of montmorillonite-rich Hapludults in the Alabama Coastal Plains. *Soil Sci.* **142**, 76–82.
- Lander, R.H. and Hay, R.L.** (1993) Hydrogeologic control on zeolite diagenesis of the White River sequence. *Geol. Soc. Am. Bull.* **105**, 361–376.
- Larson, E.E. and Evanoff, E.** (1998) Tephrostratigraphy and source of the tuffs of the White River sequence. In: *Depositional Environments, Lithostratigraphy, and Biostratigraphy of the White River and Arikaree Groups (Late Eocene to Early Miocene, North America)* (Eds D. O. Terry, H. E. Jr, LaGarry and R. M. Hunt, Jr). *Geol. Soc. Amer. Spec. Paper* **325**, 1–14.
- Lipman, P.W.** (1975) Evolution of the Platoro caldera complex and related volcanic rocks, southeastern San Juan Mountains, Colorado. *U.S. Geol. Survey Prof. Paper* 852.
- Loope, D.B.** (1986) Recognizing and utilizing vertebrate tracks in cross section: Cenozoic hoofprints from Nebraska. *Palaios*, **1**, 141–151.
- Machette, M.N.** (1985) Calcic soils of the southwestern United States. In: *Soils and Quaternary Geology of the Southwestern United States* (Ed. D. L. Weide) *Geol. Soc. Amer. Spec. Paper* **203**, 1–21.
- Mason, J.A., Milfred, C.J. and Nater, E.A.** (1994) Distinguishing parent material and soil age effects on an Ultisol of north-central Wisconsin, USA. *Geoderma*, **61**, 165–189.
- Motts, W.S.** (1965) Hydrologic types of playas and closed valleys and some relations of hydrology to playa geology. In: *Geology, Mineralogy, and Hydrology of U.S. Playas* (Ed. J. T. Neale) *U.S. Air Force Cambridge Research Laboratories, Environmental Research Papers* **96**, 73–104.
- Osterkamp, W.R. and Wood, W.W.** (1987) Playa-lake basins on the southern High Plains of Texas and New Mexico, part 1: hydrologic, geomorphic, and geologic evidence for their development. *Geol. Soc. Am. Bull.* **99**, 215–223.
- Osterkamp, W.R., Fenton, M.M., Gustavson, T.C., Hadley, R.F., Holliday, V.T., Morrison, R.B. and Toy, T.J.** (1987) Great plains. In: *Geomorphic Systems of North America* (Ed. W.L. Graf). *Geol. Soc. Amer. Centennial Spec.* **2** 163–210.
- Parat, F., Dungan, M.A. and Streck, M.J.** (2002) Anhydrite, pyrrhotite, and sulfur-rich apatite: tracing the sulfur evolution of an Oligocene andesite (Eagle Mountain, CO, USA). *Lithos*, **64**, 63–75.
- Robock, A.** (2000) Volcanic eruptions and climate. *Rev. Geophys.* **38**, 191–219.
- Rose, W.I., Bluth, G.J.S., Schneider, D.J., Ernst, G.G.J., Riley, C.M., Henderson, L.J. and McGimsey, R.G.** (2001) Observations of volcanic clouds in their first few days of atmospheric residence: the 1992 eruptions of Crater Peak, Mount Spurr Volcano, Alaska. *J. Geol.* **109**, 677–694.
- Rose, W.I., Riley, C.M. and Darteville, S.** (2003) Size and shape of 10-Ma distal fall pyroclasts in the Ogallala Group. *J. Geol.* **111**, 115–124.
- Schenk, C.J.** (1990) Eolian deposits of the Ojo Caliente Sandstone Member (Miocene) of the Tesuque Formation, Espanola Basin, New Mexico. In: *Modern and Ancient Eolian Deposits: Petroleum Exploration and Production* (S.G. Fryberger, L.F. Krystinik, and C.J. Schenk). Rocky Mountain Section, S.E.P.M., Denver, CO, 18–1–18–9.
- Stanley, K.O. and Benson, L.V.** (1979) Early diagenesis of High Plains Tertiary vitric and arkosic sandstone, Wyoming and Nebraska. In: *Aspects of Diagenesis* (Eds P. A. Scholle and P. R. Schluter). *SEPM. Spec. Publ.* **26**, 401–423.
- Stephens, D.B.** (1996) *Vadose Zone Hydrology*. CRC Press, Boca Raton, Florida.
- Stoffregen, R.** (1987) Genesis of acid-sulfate alteration and Au-Cu-Ag mineralization at Summitville, Colorado. *Economic Geol.* **82**, 1575–1591.
- Stothers, R.B.** (1984) The great Tambora eruption in 1815 and its aftermath. *Science*, **224**, 1191–1198.
- Stothers, R.B.** (1996) The great dry fog of 1783. *Climate Change*, **32**, 79–89.
- Swinehart, J.B. and Loope, D.B.** (1987) Late Cenozoic geology of the summit to museum trail, Scotts Bluff National Monument, Nebraska. In: *North Central Section of the Geological Society of America* (Ed. D. L. Biggs) *Centennial Field Guide* **3**, 13–18.
- Swinehart, J.B., Souders, V.L., DeGraw, H.M. and Diffendal, R.F.** (1985) Cenozoic paleogeography of western Nebraska. In: *Cenozoic Paleogeography of West-Central United States*



- (Eds R. M. Flores and S. S. Kaplan). pp. 209–229. Rocky Mountain Section, SEPM, Denver, CO.
- Tedford, R.H., Swinehart, J.B., Swisher, C.C. III, Prothero, D.R., King, S.A. and Tierney, T.E.** (1996) The Whitneyan-Arikareean transition in the High Plains. In: *The Terrestrial Eocene-Oligocene Transition in North America* (Eds D. R. Prothero and R. J. Emry). pp. 312–334. Cambridge University Press, Cambridge.
- Terry, D.O., LaGarry, H.E. and Hunt, R.M. Jr,** eds. (1998) Depositional Environments, Lithostratigraphy, and Biostratigraphy of the White River and Arikaree Groups. *Geol. Soc. Amer. Spec. Paper* 325.
- Thordarson, T. and Self, S.** (1996) Sulfur, chlorine, and fluorine degassing and atmospheric loading by the Roza eruption, Columbia River Basalt Group, Washington, USA. *J. Volcanol. Geothermal Res.* **74**, 49–73.
- Thordarson, T. and Self, S.** (2003) Atmospheric and environmental effects of the 1783–1784 Laki eruption: a review and reassessment. *J. Geophys. Res.* **108** (D1), 4011.
- Thordarson, T., Self, S., Miller, D.J., Larsen, G. and Vilmundardottir, E.G.** (2003) Sulfur release from flood lava eruptions in the Veidivotn, Grimsvotn and Katla volcanic systems, Iceland. In: *Volcanic Degassing* (Eds C. Oppenheimer, D. M. Pyle and J. Barclay) *Geol. Soc. London. Spec. Publ.* **213**, 103–121.
- Warren, J.K.** (1989) *Evaporite Sedimentology*. Prentice Hall, Englewood Cliffs, NJ.
- Washburn, A.L.** (1973) *Periglacial Processes and Environments*. Edward Arnold, London.
- Watson, A.** (1983) Gypsum crusts. In: *Chemical Sediments and Geomorphology* (Eds Goudie and K. Pye). pp. 133–161. Academic Press, London.
- Wilding, L.P. and Tessier, D.** (1988) Genesis of vertisols: shrink-swell phenomena. In: *Vertisols: Their Distribution, Properties, Classification, and Management* (Eds L. P. Wilding and R. Puentes). *Soil Management Support Services, Technical Monograph no. 18*, pp. 55–81. Texas A & M University Printing Center.
- Yasui, M., Fujiwara, M., Shibata, T., Akiyoshi, H., Ikawa, S., Shiraishi, K. and Nonaka, H.** (1996) Variations of volcanic aerosols observed in Fujioka- a comparison of Mt. El Chichon and Mt. Pinatubo events. *J. Geomagnetism Geoelectricity*, **48**, 403–413.

*Manuscript received 25 September 2003;  
revision accepted 11 August 2004.*